RESEARCH MEMORANDUM

PERFORMANCE CHARACTERISTICS OF A NORMAL-SHOCK SIDE INLET LOCATED DOWNSTREAM OF A CANARD CONTROL SURFACE AT MACH NUMBERS OF 1.5 AND 1.8

By Murray Dryer and Andrew Beke

Lewis Flight Propulsion Laboratory
Cleveland, Ohio

NATIONAL ADVISORY COMMITTEE
FOR AERONAUTICS

WASHINGTON

July 29, 1952

NATIONAL ADVISORY COMMITTEE FOR AERONAUTICS

RESEARCH MEMORANDUM

PERFORMANCE CHARACTERISTICS OF A NORMAL-SHOCK SIDE INLET LOCATED DOWNSTREAM OF A CANARD CONTROL SURFACE AT MACH NUMBERS OF 1.5 AND 1.8

By Murray Dryer and Andrew Beke

SUMMARY

The performance of a normal-shock side inlet located behind a triangular control surface is presented for a range of angles of attack, control surface deflections, and a -3° angle of yaw at Mach numbers of 1.5 and 1.8. Several ram-type boundary-layer removal systems were considered for a limited range of operation. Data were also obtained with the control surface removed.

An increase of 1 to 3 percent in total pressure recovery at the diffuser exit (engine face) was accomplished by a slight modification of the original bleed system. Further reduction in the amount of boundary-layer air entering the inlet by increasing the bleed height resulted in an additional increase of 1 to 3 percent in total pressure recovery when the local flow was oblique to the inlet. The diffuser performance remained insensitive to increased boundary-layer removal when the flow was alined with the inlet axis.

The largest losses in total pressure recovery associated with the control-surface vortex wake occurred at zero body angle of attack. This effect was less pronounced as the angle of attack was increased above 6°. The total pressure losses minimized at approximately 6° angle of attack because of the 6° downward cant of the inlet axis with respect to the fuselage axis. For a -3° adverse angle of yaw and zero control surface deflection, the total pressure recovery decreased about 1 to 5 percent for the range of angles of attack investigated. The total pressure recoveries obtained for the entire range of variables were below theoretical normal-shock recovery.

INTRODUCTION

Several recent studies of the flow field behind a canard control surface (references 1 to 3) have indicated the importance of considering the influence of the shed vortex sheet on the region adjacent to the fuselage of a supersonic aircraft. These shed vortices alter the potential flow field about the body and result in total pressure losses, flow direction irregularities, and a redistribution of the boundary layer. It is the purpose of this investigation to determine the severity of restrictions thereby imposed on the aerodynamic characteristics of a normal-shock-type side (or scoop) air inlet located in or near these regions.

The performance of a normal-shock-type side inlet located downstream of a triangular control surface is presented at Mach numbers of 1.5 and 1.8 for a range of angles of attack from 0° to 12°; control-surface deflections of 0°, 5°, and 10°; and for a yaw angle of -3°. Several boundary-layer removal systems are considered for a limited range of operation. Mass flow requirements of a hypothetical turbojet engine are used in some instances as a basis for comparisons of duct performance. A brief breakdown of losses in total pressure recovery is also presented. The experimental investigation was conducted in the NACA Lewis 8- by 6-foot supersonic tunnel at a Reynolds number of approximately 16×10^6 based on forebody length ahead of the inlet.

SYMBOLS

A	duct cross-sectional area normal to center line of flow
P	total pressure
M	Mach number
m	mass flow
$\bar{p}$	average static pressure
m_1/m_0	ratio of mass flow at given condition to mass flow in free stream having an area equal to inlet area
α	angle of attack with respect to free stream (deg)
δ	control-surface deflection with respect to longitudinal body axis (deg)
ψ	angle of yaw (deg)

Subscripts:

0	free stream
1	diffuser inlet
2	double-entry engine face
3	duct exit
B	body
L	local

APPARATUS AND PROCEDURE

The test model (fig. 1) consisted of a body of revolution with a side air inlet located 2.14 mean aerodynamic chord lengths behind the trailing edge of a triangular control surface. The control surface had a leading-edge sweep angle of 30°, dihedral of 15°, and a span of 15 inches. The air induction system comprised a sharp-lip normal-shock entrance, a subsonic diffuser, and a boundary-layer scoop located forward of the entrance lip.

The axis of the diffuser inlet section was canted 6° downward with respect to the body longitudinal axis, as shown in figure 2. This angle of cant was selected to permit approximate alinement of the inlet with the free stream at a hypothetical cruise angle of attack of 6°. The center line of the inlet was located 25° below the body cross-sectional horizontal axis. The duct shape varied from a semicircular section at the inlet (station 44.66) to a circular section (station 56.10) ahead of a strut, which split the diffuser into equal elliptical sections to simulate the double-entry engine face (station 61.23). The duct area variation normal to the center line of the flow is shown in figure 3, and a view of the inlet is shown in figure 4.

The original boundary-layer scoop, which was located 0.94 inch forward of the inlet entrance, had a bleed height of 0.24 inch. Boundary-layer mass flow was ducted to the free stream through five diverging channels of quadrilateral cross section, as shown in figure 5(a). In order to decrease the amount of boundary-layer air entering the inlet, modifications of the original bleed system (fig. 5(a)) were made as follows: (1) a 0.10-inch cutback of the ramp lip and a 0.52-inch cutback of the internal guide vanes (modification 1, fig. 5(b)), and (2) removal of the internal vanes and substitution of the bleed base block with one which had local reductions of body radii resulting in an effective

bleed height of 0.42 inch (modification 2, fig. 5(c)). The increased bleed height for the latter change was determined from boundary-layer rake data taken on the right side of the body for the maximum boundary-layer thickness at the inlet station obtained with zero control surface deflection.

Control surface deflection angles of 0°, 5°, and 10° were obtained by using removable adapter blocks fitted to the control surfaces. Smooth body-contoured blocks were inserted to obtain data without the control surface.

The model was mounted on a sting which had an offset angle of 3° in the pitch plane. Rotating the sting 90° permitted angle of attack investigation in combination with 3° of yaw.

Total pressure measurements were made at the duct inlet (station 1), engine face (station 2), and the exit (station 3), as shown in figure 2. The inlet rakes were not installed when total pressures were recorded at the engine face. Mean total pressures recorded at the engine face are the area-integrated total pressures measured at the inboard and outboard engine faces at station 2. Three pitot tubes and static orifices were located on the floor of the duct (fig. 2) for the detection of flow separation. A static pressure pick-up, located between stations 2 and 3, was connected to a pressure-time recorder for the detection of pulsing phenomena. Local Mach numbers at the inlet station were determined from survey rake data obtained at the inlet station on the right side of the model. Since the purpose of the investigation was primarily to study internal flow characteristics, no force measurements were made.

Main duct mass flow, which was varied by means of a translating conical plug at the duct exit, was determined from integrated total pressures at the exit station and plug exit areas based on choked flow at the minimum area. The mass flow ratios were based on free-stream conditions; therefore, ratios of 1.0 were not obtained because inlet conditions did not correspond to free-stream conditions.

In order to establish a realistic criterion for comparisons of diffuser characteristics at a fixed operating condition for the range of test variables, an analysis of a turbojet engine-inlet matching problem was performed using the method of reference 4 together with the assumed required corrected weight flows for a hypothetical turbojet engine. Accordingly, figure 6 shows the variation of the engine operating line with diffuser pressure recovery at $M_0 = 1.5$ and 1.8. Thus, for a given air induction system, the engine will be supplied the necessary mass flow for a required flight Mach number, altitude (in the tropopause), and at rated engine speed when the total-pressure-recovery mass-flow relationship for the inlet-diffuser system intersects the engine operation curve. Comparisons of the diffuser characteristics are therefore made at this condition in some instances.

RESULTS AND DISCUSSION

Boundary-Layer Bleed Investigation

To determine the effect of boundary-layer removal on performance of a normal-shock-type inlet, the test was initiated with an investigation of several bleed systems at zero control surface deflection. A body angle of attack of 3° was arbitrarily selected to enable schlieren observation of the inlet. The boundary-layer profiles at the inlet station (fig. 7) give an indication of the amount of boundary-layer air entering the scoop for the original bleed height of 0.24 inch. Removal of additional boundary-layer mass flow was accomplished by increasing the bleed height from 0.24 inch to 0.42 inch (modification 2, fig. 5(c)). A comparison of total pressure recovery at the engine face for modifications 1 and 2 is presented in figures 8(a) and 8(b) for $M_0 = 1.5$ and 1.8, respectively, for the range of angles of attack; the results obtained with the original bleed system are shown for $\alpha_B = 3^\circ$ only. As seen in figure 8(b) from the 1 to 3 percent increase in total pressure recovery at the engine face for all duct mass flow ratios modification 1 (at $M_0 = 1.8$; $\alpha_B = 3^\circ$) effectively increased the bleed mass flow. Modification 2 further increased the total pressure recovery on the order of 1 to 3 percent for all angles of attack except the cruise angle of 6° where the increase was negligible. The increases of local Mach number due to the reduction of body radii at the inlet station apparently had little effect. However, estimates indicate that additional gains of the order of 1 to 2 percent in pressure recovery for each angle of attack could have been realized had the boundary-layer bleed height been increased and the original body contour maintained. The relative insensitivity of the diffuser performance at $\alpha_B = 6^\circ$ is probably due to the 6° downward cant of the inlet axis with respect to the body longitudinal axis resulting in local flow alinement with the inlet axis

Flow Characteristics at Engine Intakes

Characteristics of the flow at the engine twin intake faces are presented (fig. 9) in the form of contours of total pressure recovery for the condition of 95 percent of the engine rated mass flow. It is seen that the variation of total pressure recovery in each elliptical duct was 3 to 4 percent at $\alpha_B = 0$ and 8 to 10 percent at $\alpha_B = 12^\circ$. As might be expected from inspection of the duct geometry in figure 2, the high energy flow in the outboard engine face at all angles of attack was concentrated along the splitter strut. On the other hand, the high energy flow in the inboard engine face moved from the side of the splitter strut at $\alpha_B = 0$ to the upper half of the engine face at $\alpha_B = 12^\circ$. These total pressure contours are representative of the entire range of variables investigated. Mach number profiles may be obtained directly from the ratios of static to total pressure given in the table in figure 9.

Duct Performance with Bleed System of Modification 1

Although the total pressure recoveries obtained with modification 2 were somewhat higher than those obtained with modification 1 for most angles of attack, the diffuser performance was the same for both modifications at the cruise condition, $\alpha_B = 6^\circ$. Therefore, the major portion of the data was obtained with the bleed system of modification 1. Accordingly, the duct performance is presented and compared for various conditions of angle of attack, control surface deflection, and, to some extent, yaw.

Zero angle of yaw. - The effect of angle of attack and control surface deflection on the flow conditions at the inlet face without inlet or boundary-layer bleed in place are reproduced from reference 1 in figure 10. These contours of local total pressure recovery indicate that for $\delta = 0$ the effect of the shed vortex sheet on the body boundary layer was very small at angles of attack of 0 and 6°. However, the vortex sheet resulting from deflection of the control surface for these body attitudes appreciably increased the quantity of low energy air ahead of the inlet by redistributing the body boundary-layer air. The ensuing effect on total pressure recovery at the engine face is shown at $M_0 = 1.5$ (fig. 11(a)) and $M_0 = 1.8$ (fig. 11(b)) for the range of angles of attack and control surface deflections. The results at $\delta = 0$ are significantly the same as those obtained with the control surface removed. This condition could be expected from inspection of the similar flow conditions at the inlet (fig. 10), which show that the inlet is below the region affected by the combination of the body cross flow and the control surface wake. As shown by the dashed lines in figure 11, pulsing occurred in the low range of mass flow ratios (roughly, $m_1/m_0 < 0.75$) at control surface deflections of 5° and 10°. Although the occurrence of pulsing is inconsistent, there is some correspondence between pulsing and the complex flow in the vicinity of the inlet at $\alpha_B = 3^\circ$ and $\delta = 5^\circ$ and 10°. In general, it is seen from figure 11 that increasing the control surface deflection at $\alpha_B = 0$ caused the largest decrease in total pressure recovery due to the influence of the shed vortex sheet on the boundary layer; as the angle of attack was increased above 6° the effect of control surface deflection was negligible.

The engine operating condition for a hypothetical turbojet engine is shown in figures 11(a) and 11(b). A summary of the total pressure recoveries at this condition is presented in figure 12 for $M_0 = 1.5$ and 1.8. The highest total pressure recoveries were obtained at an angle of attack of 6° for nearly the entire range of control surface deflections. The total pressure recovery remained nearly constant at about 87 percent at $M_0 = 1.5$ and about 75 percent at $M_0 = 1.8$ up to $\delta = 5^\circ$. Further increases in control surface deflection resulted in a decrease in total pressure recovery. For angles of attack less than approximately 6°, the total pressure recovery steadily decreased with increasing control

surface deflections; whereas, for angles of attack greater than about 6°, the total pressure recovery was independent of the control surface deflections. This result might be anticipated from inspection of figure 10, which shows that the flow conditions at the inlet are independent of control surface deflections at angles of attack greater than 6°.

A breakdown of the total pressure recovery losses is presented in figure 13 for $m_1/m_0 = 0.90$ at $\delta = 0$. The inlet and subsonic diffuser losses minimized at about $\alpha_B = 6°$ for the range of angles of attack. A major portion of losses occurring at the inlet was due to high local Mach numbers. At $\alpha_B = 12°$ the local inlet Mach numbers exceeded the free-stream Mach number by a maximum of 8 percent at $M_0 = 1.5$ and 9.5 percent at $M_0 = 1.8$. The resulting normal shock losses therefore increased with angle of attack. Large inlet losses are also attributed to the flow separation which resulted from normal-shock boundary-layer interaction on the ramp as well as lip angularity near the ramp with respect to the local flow direction. Data from an inlet survey indicated a movement of the separated region from the upper section of the inlet at $\alpha_B = 0$, to a minimum region along the ramp at $\alpha_B = 6°$, and then to a large region at the lower section of the inlet at $\alpha_B = 12°$. The subsonic diffusion losses were relatively small up to an angle of attack of the order of 6° at both Mach numbers, as shown in figure 13, and then increased appreciably with increasing angle of attack. At the low angles of attack, the flow evidently reattached rather quickly, but at the higher angles of attack, the flow remained separated for at least 10 inches downstream of the inlet, as indicated by the pitot tube and static orifices instrumentation (fig. 2). The diffusion that resulted from this latter condition is shown (fig. 9) by engine-face total pressure contours in the form of low total pressure recoveries in the lower half of the inboard engine face. The major portion of the over-all losses, however, was due to separation on the ramp and occurrence of the normal shock at a local inlet Mach number which exceeded M_0. In general, it is noted that the highest total pressure recoveries occurred at $\alpha_B \approx 6°$, presumably as a result of minimum flow separation at the inlet and optimum angle-of-attack operation. This optimum angle of attack was directly due to the 6° downward cant of the inlet center line which resulted in an effective inlet angle of attack of approximately zero. Furthermore, it can be seen from figures 11 and 13 that theoretical normal-shock recovery was not obtained for the entire range of variables investigated.

Angle of yaw of -3°. - Variation of total pressure recovery at the engine face with mass flow ratio at $M_0 = 1.5$ and 1.8 were obtained at an adverse angle of yaw of -3° at $\delta = 0$. Some data were also obtained at $\delta = 5°$ for $M_0 = 1.8$. The characteristics of these variations were similar to those obtained at zero yaw (fig. 11) and are not presented. Instead, a summary of adverse yaw effect is presented in figure 14 for the engine operating condition and is representative of the higher mass

flow ratios ($m_1/m_0 > 0.80$). A comparison with zero yaw shows a reduction in total pressure recovery of about 1 to 3 percent for $M_0 = 1.5$ and 2 to 5 percent for $M_0 = 1.8$ for the range of angles of attack. At $M_0 = 1.8$, deflection of the control surface to 5° further decreased the total pressure recovery at angles of attack less than 6°. At an angle of attack of about 6°, the effect of this control deflection was negligible for the adverse yaw condition. The flow pattern in the form of total pressure contours at the engine face at 95 percent of the engine operating condition was substantially the same as that experienced at zero yaw; the magnitudes, however, were lower. Pulsing due to yaw occurred at the lower mass flow ratios ($m_1/m_0 < 0.75$) at $\alpha_B = 0$ and for both control deflections, presumably as a result of interaction of the body cross flow with the vortex sheet.

SUMMARY OF RESULTS

An experimental investigation of a normal-shock-type side inlet located 2.14 mean aerodynamic chord lengths behind a canard control surface was conducted with several boundary-layer-bleed modifications. From operation over a range of angles of attack, control surface deflections, and yaw for a range of main duct mass flow ratios, the following results were obtained:

1. A 1 to 3 percent increase in total pressure recovery at the engine face was obtained at $M_0 = 1.8$ and a body angle of attack of 3° by an apparent increase of the bleed mass flow accomplished with a slight modification of the original boundary-layer-bleed entrance.

2. Decreasing the amount of boundary-layer air entering the inlet by increasing the bleed height resulted in an additional increase of 1 to 3 percent in total pressure recovery when the local flow was oblique to the inlet. However, the diffuser performance was insensitive to the increased boundary-layer removal when the flow was alined with the inlet axis.

3. The largest total pressure losses associated with the wake behind the control surface occurred at a zero body angle of attack as the control surface deflection was increased from 0° to 10°. As the angle of attack was increased above 6°, the effect of increasing control surface deflection was negligible because of the passing of the wake above the inlet. At a hypothetical engine operating condition for a -3° adverse angle of yaw and zero control surface deflection, the total pressure recovery decreased about 1 to 5 percent over the range of angles of attack investigated.

4. Theoretical normal-shock total pressure recovery was not obtained for the entire range of variables investigated. The total pressure losses

were a minimum at a body angle of attack of 6°, presumably as a result of an effective inlet angle of attack of zero degrees.

Lewis Flight Propulsion Laboratory
National Advisory Committee for Aeronautics
Cleveland, Ohio

REFERENCES

1. Wise George A., and Dryer, Murray: Influence of a Canard-Type Control Surface on Flow Field in Vicinity of Symmetrical Fuselage at Mach Numbers 1.8 and 2.0. NACA RM E52E13, 1952.

2. Fradenburgh, Evan A., Obery, Leonard J., and Mello, John F.: Influence of Fuselage and Canard-Type Control Surface on the Flow Field Adjacent to a Rearward Fuselage Station at a Mach Number of 2.0 - Data Presentation. NACA RM E51K05, 1952.

3. Wetzel, Benton, E., and Pfyl, Frank A.: Measurements of Downwash and Sidewash Behind Cruciform Triangular Wings at Mach Number 1.4. NACA RM A51B20, 1951.

4. Schueller, Carl F., and Esenwein, Fred T.: Analytical and Experimental Investigation of Inlet-Engine Matching for Turbojet-Powered Aircraft at Mach Numbers up to 2.0. NACA RM E51K20, 1952.

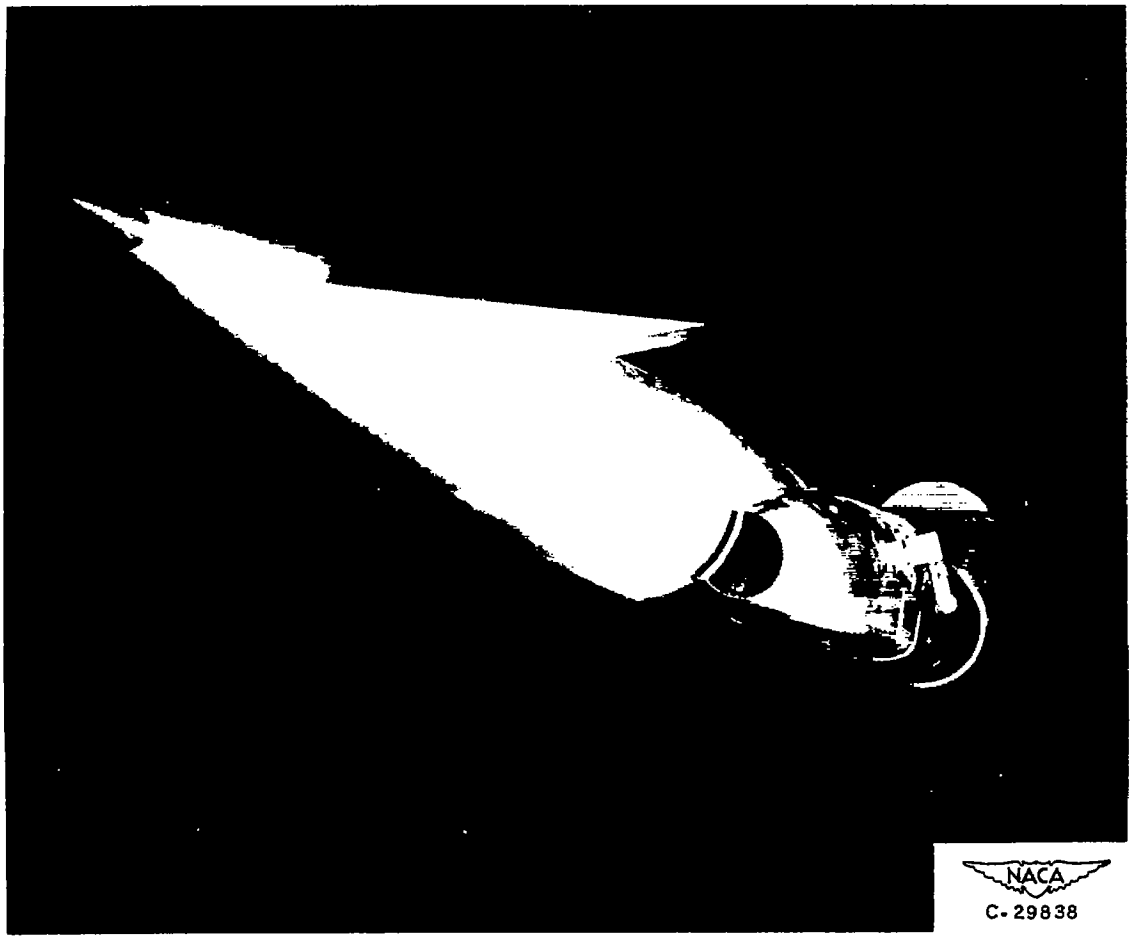

Figure 1. - Inlet-body-control surface configuration mounted in 8- by 6-foot supersonic tunnel. Inlet survey rake removed.

Body coordinates	
Station	Diameter
0	0
6.27	1.94
11.77	3.42
17.27	4.84
22.77	5.87
28.27	6.48
33.77	7.02
39.27	7.36
44.77	7.48

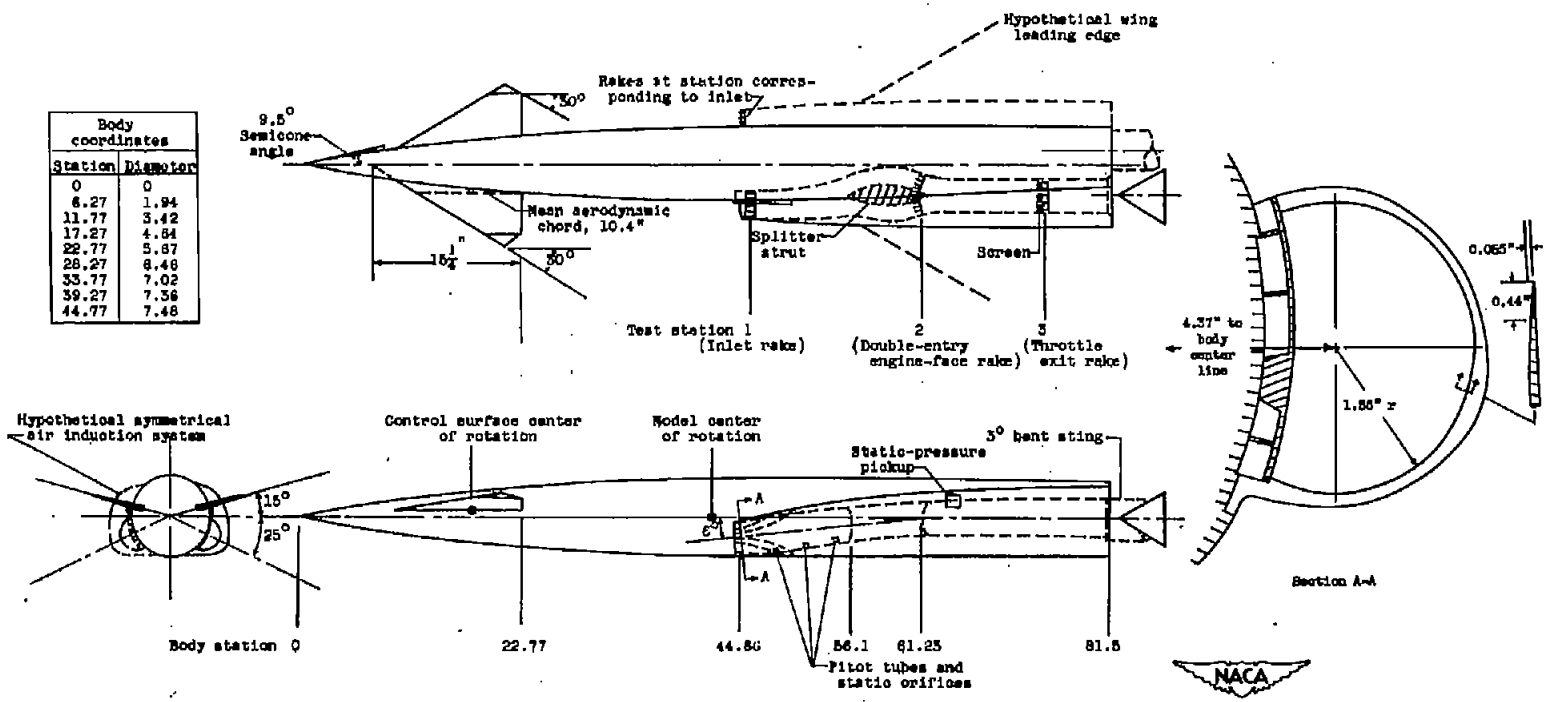

Figure 2. - Schematic drawing of test model showing normal-shock side inlet and subsonic diffuser.

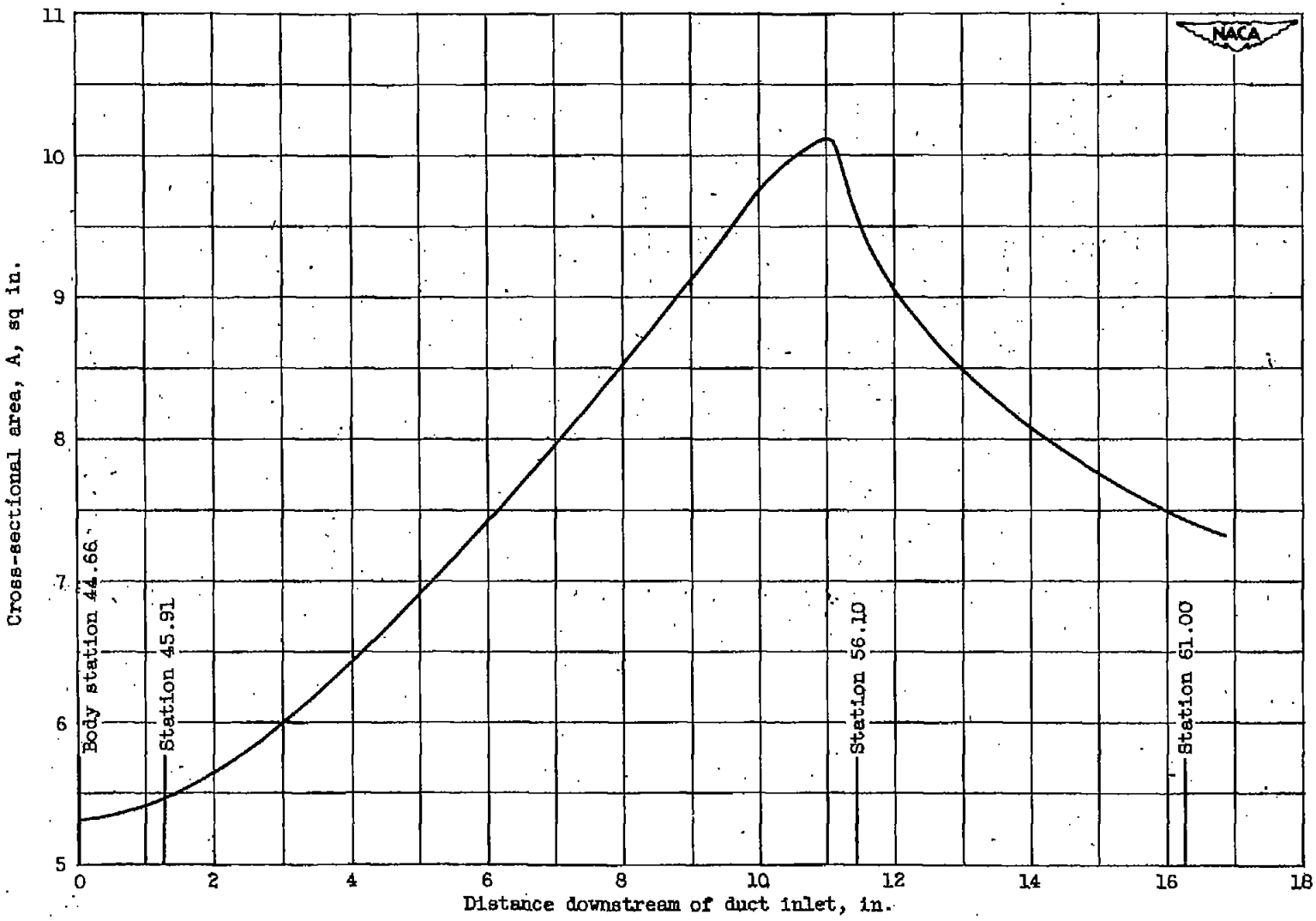

Figure 3. - Variation of duct cross-sectional area (normal to center line of flow) with distance downstream of inlet.

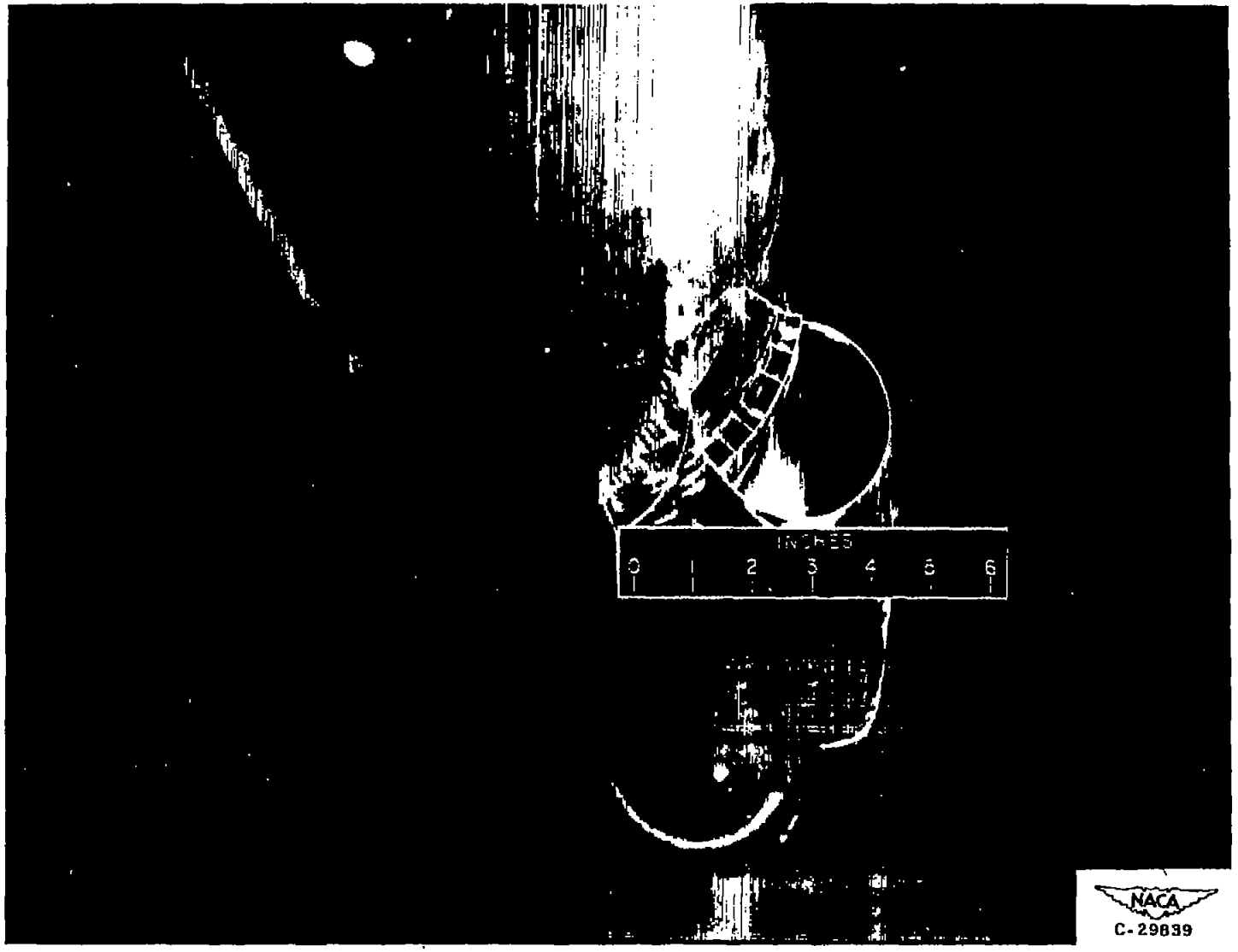

Figure 4. - Close-up view of inlet showing boundary-layer-bleed vanes and duct splitter strut.

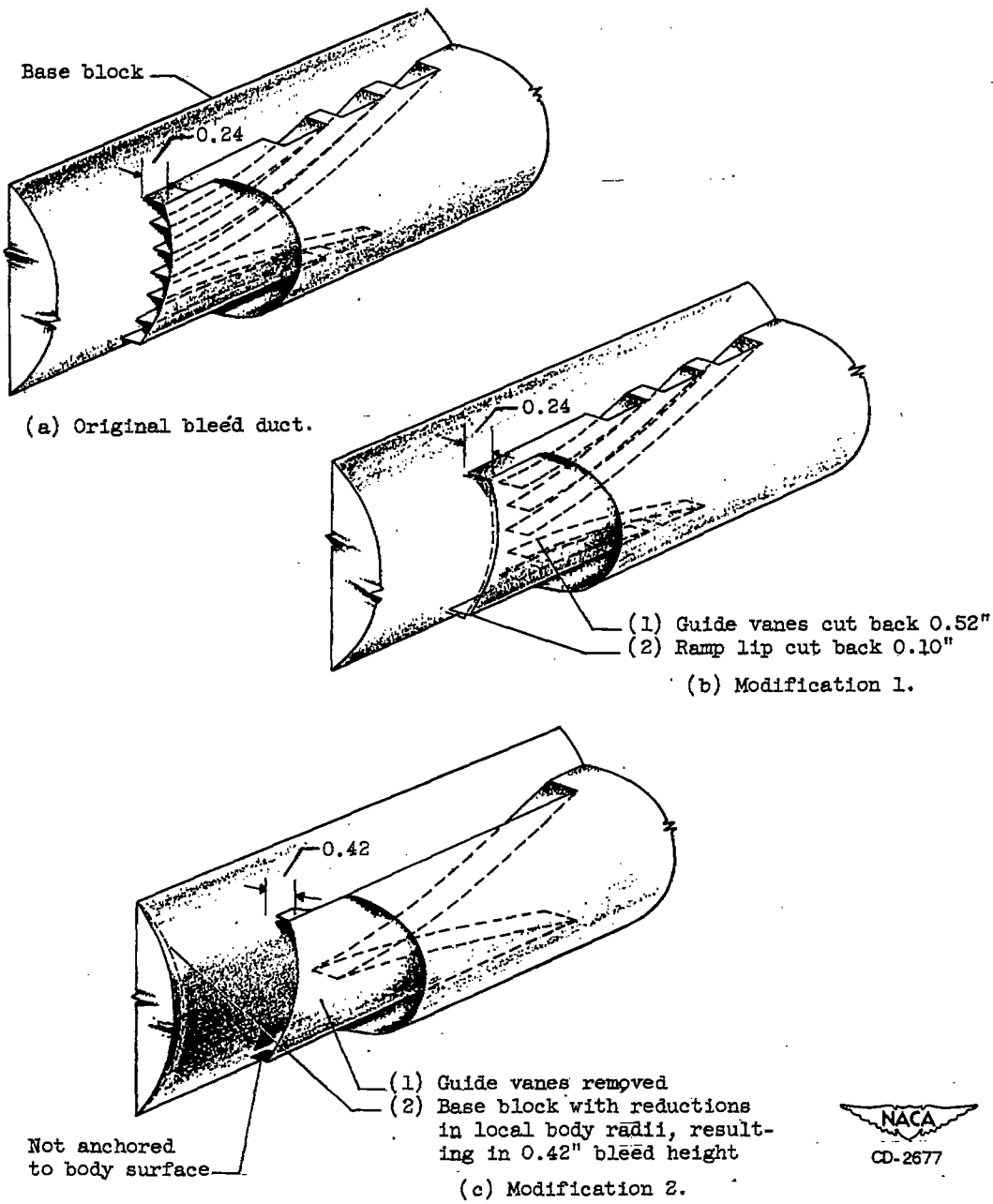

Figure 5. - Schematic drawing of boundary-layer-bleed duct and its modifications. (All dimensions are given in inches.)

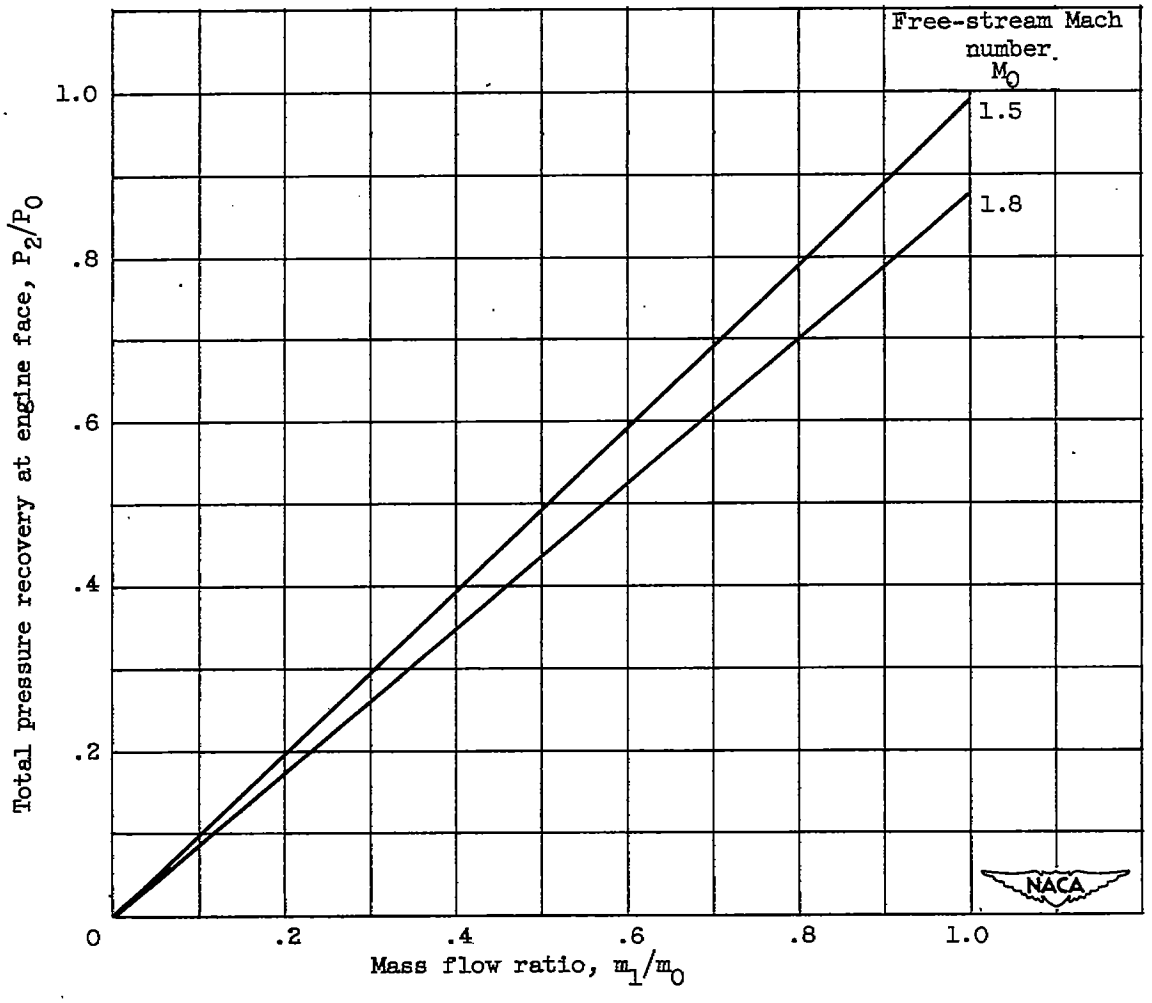

Figure 6. - Engine operating lines for given altitude (tropopause) and hypothetical turbojet engine (at rated engine speed).

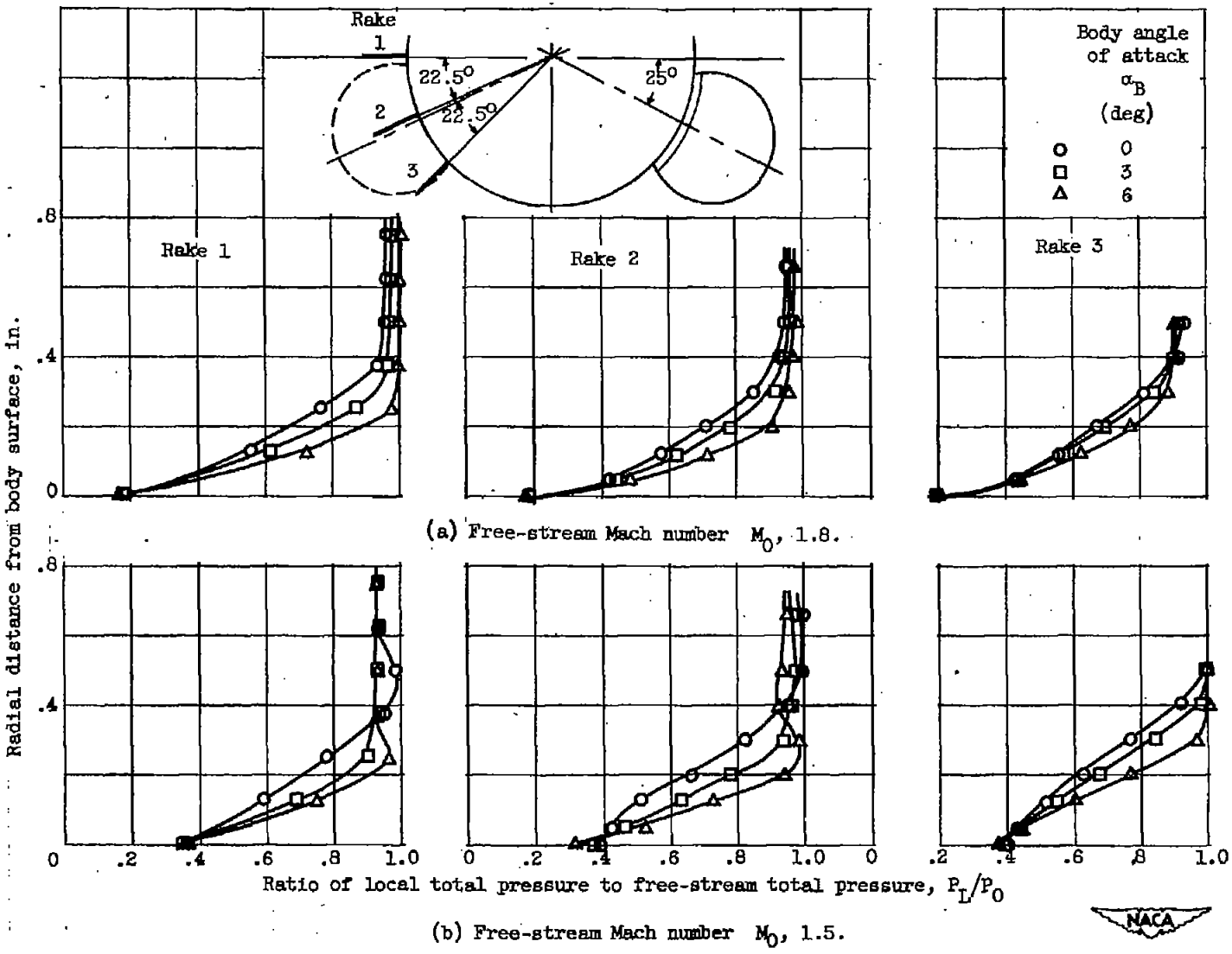

(a) Free-stream Mach number M_0, 1.8.

(b) Free-stream Mach number M_0, 1.5.

Figure 7. - Boundary-layer profiles at inlet station. Control surface deflection δ, 0.

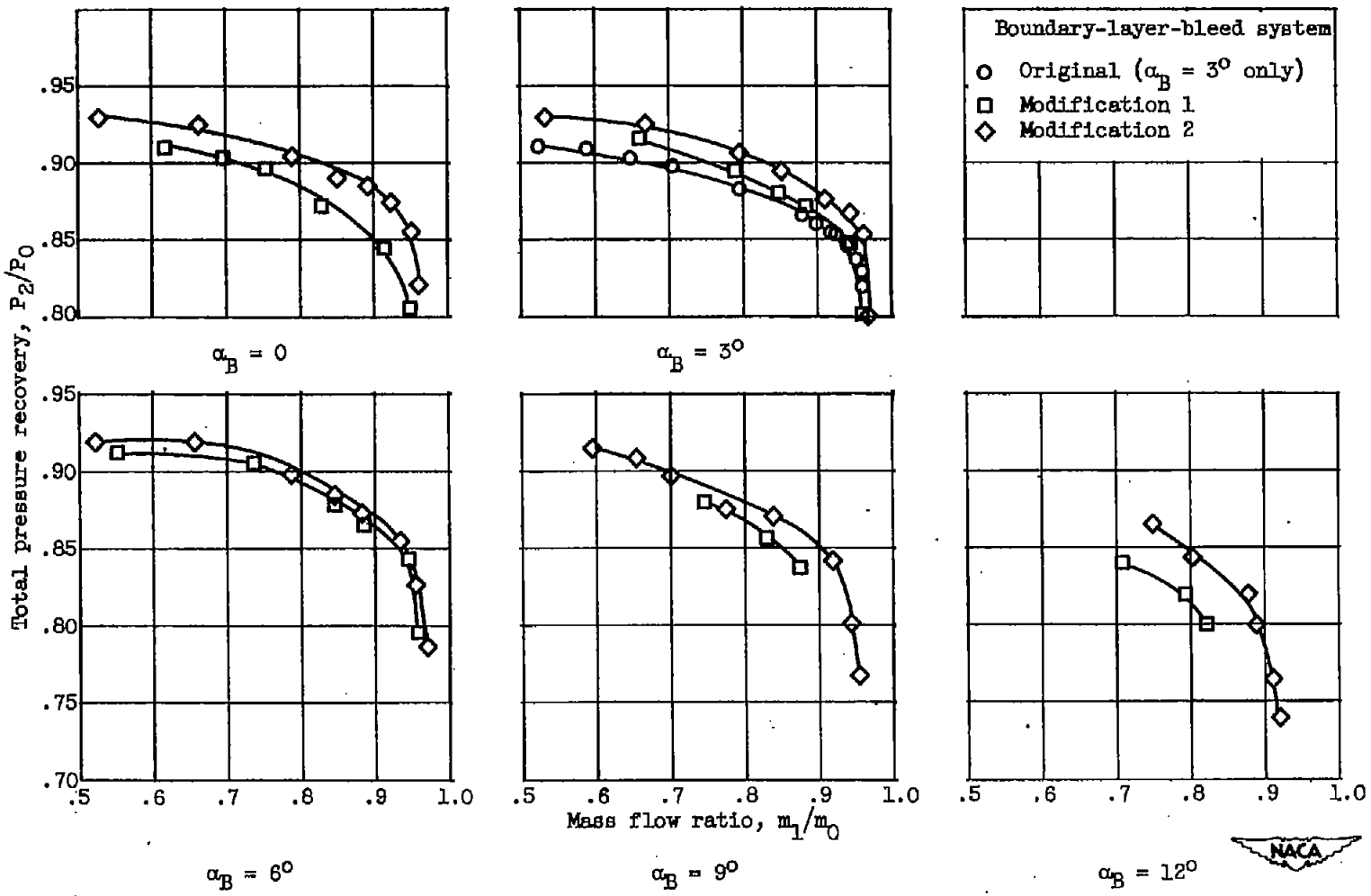

(a) Free-stream Mach number M_0, 1.5.

Figure 8. - Total-pressure-recovery mass-flow relationships for various boundary-layer-bleed systems. Control surface deflection δ, 0.

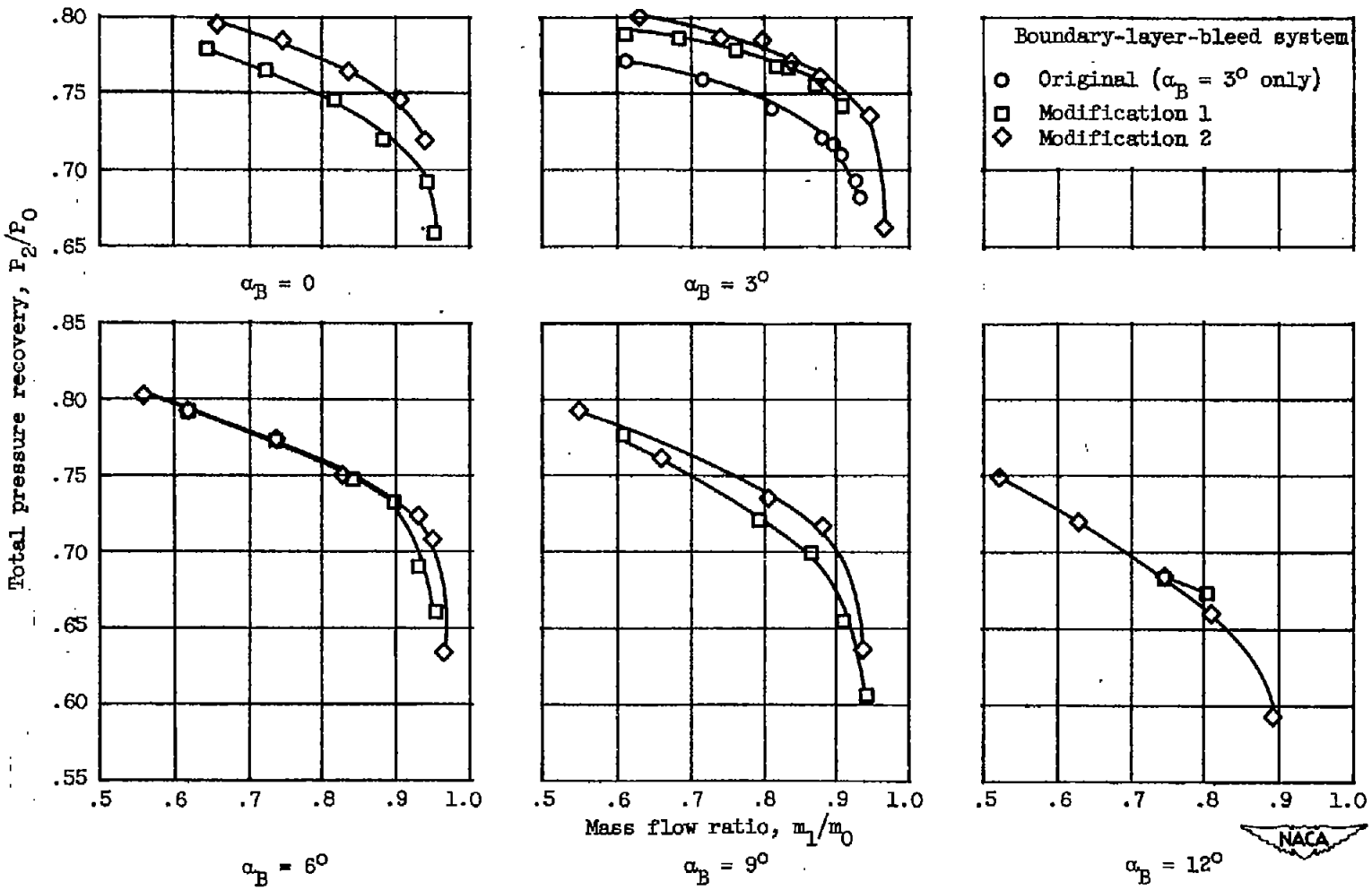

(b) Free-stream Mach number M_0, 1.8.

Figure 8. - Concluded. Total-pressure-recovery mass-flow relationships for various boundary-layer-bleed systems. Control surface deflection δ, 0.

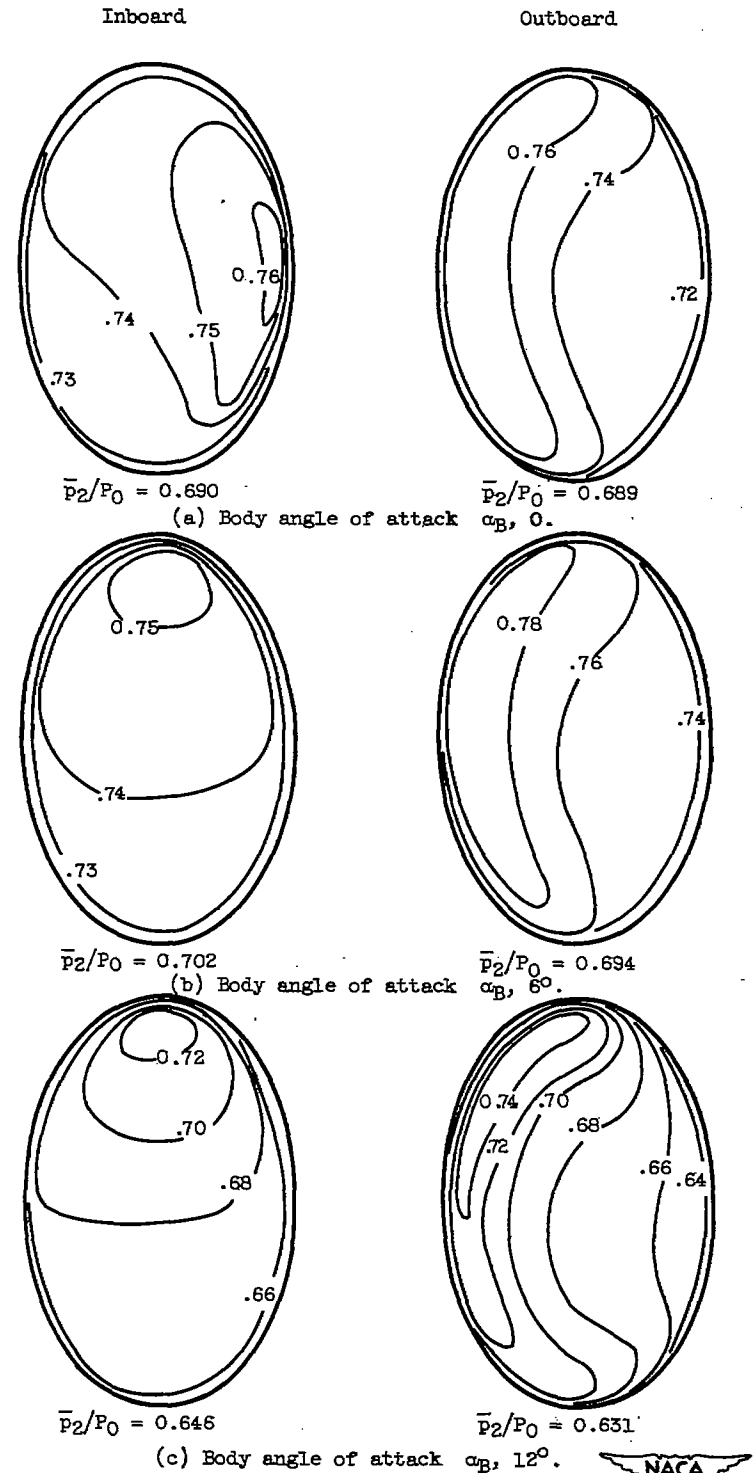

Figure 9. - Contours of total pressure recovery at engine twin intake faces at 0.95 engine rated mass flow. Free-stream Mach number M_0, 1.8; control surface deflection δ, 0; angle of yaw ψ, 0.

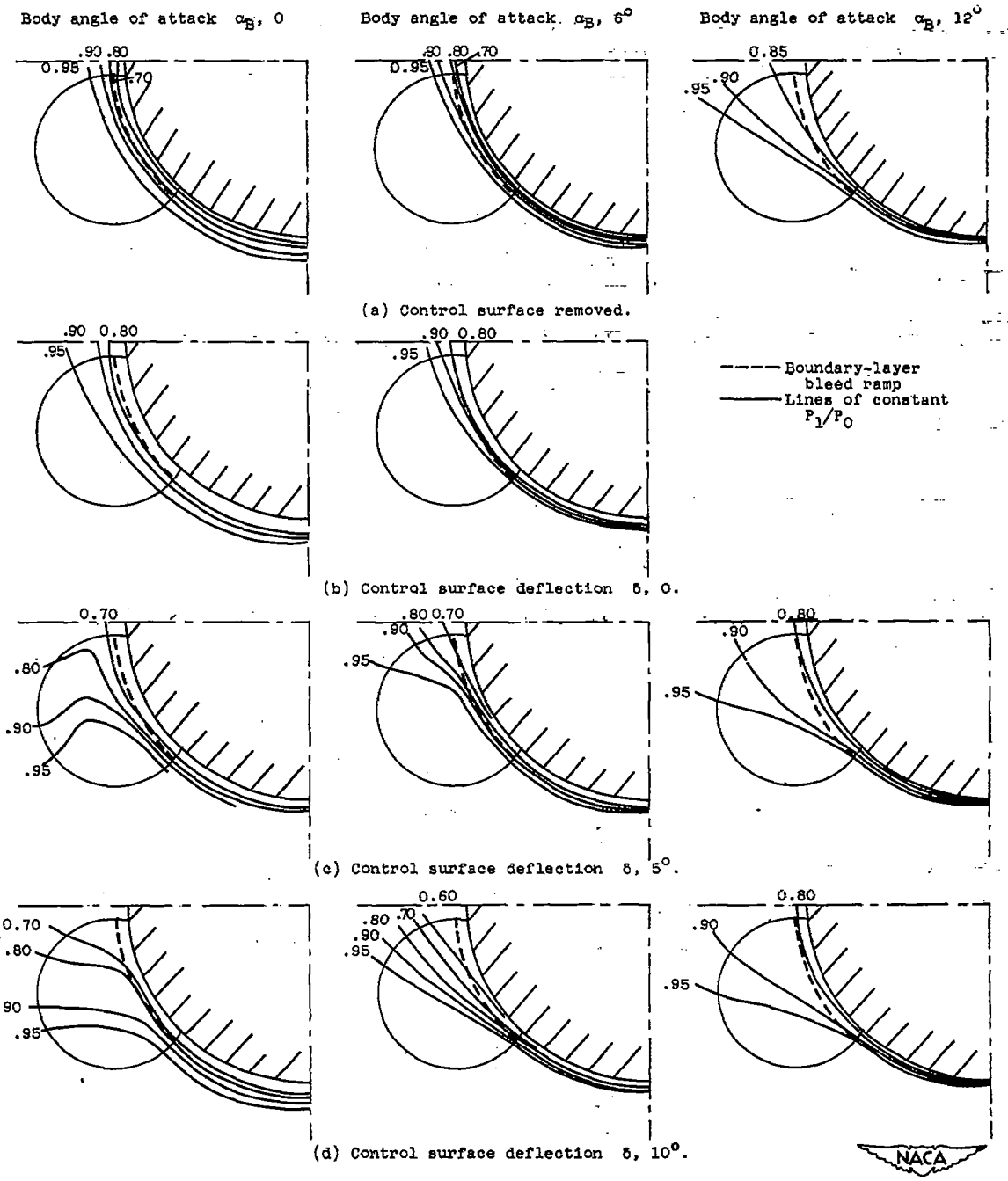

Figure 10. - Contours of total pressure recovery P_1/P_0 at normal-shock inlet. Free-stream Mach number M_0, 1.8. (Data obtained from reference 1; data not obtained for $\alpha_B = 12°$, $\delta = 0$.)

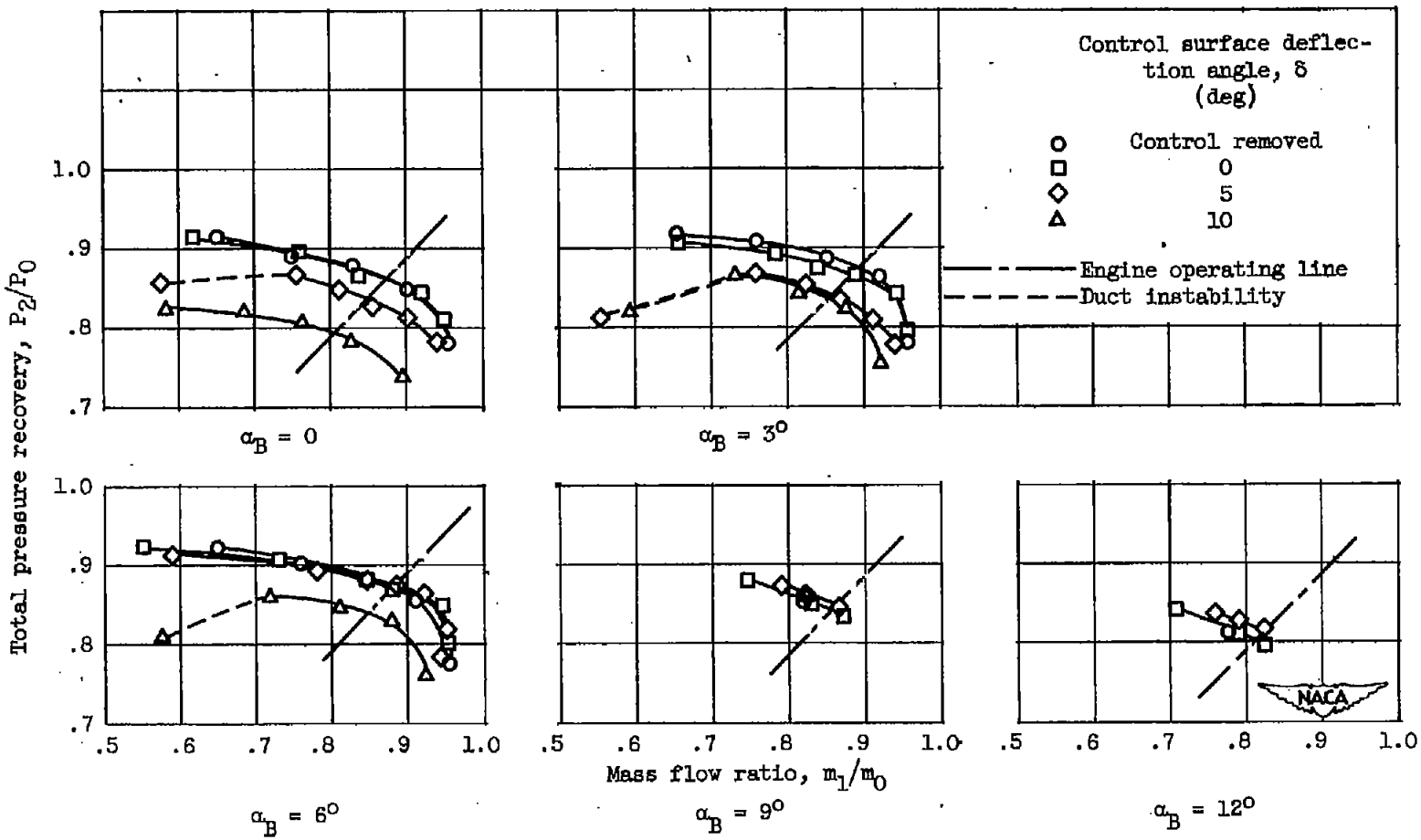

(a) Free-stream Mach number M_0, 1.3.

Figure 11. - Total-pressure-recovery mass-flow relationships for various control surface deflection angles. Angle of yaw Ψ, 0.

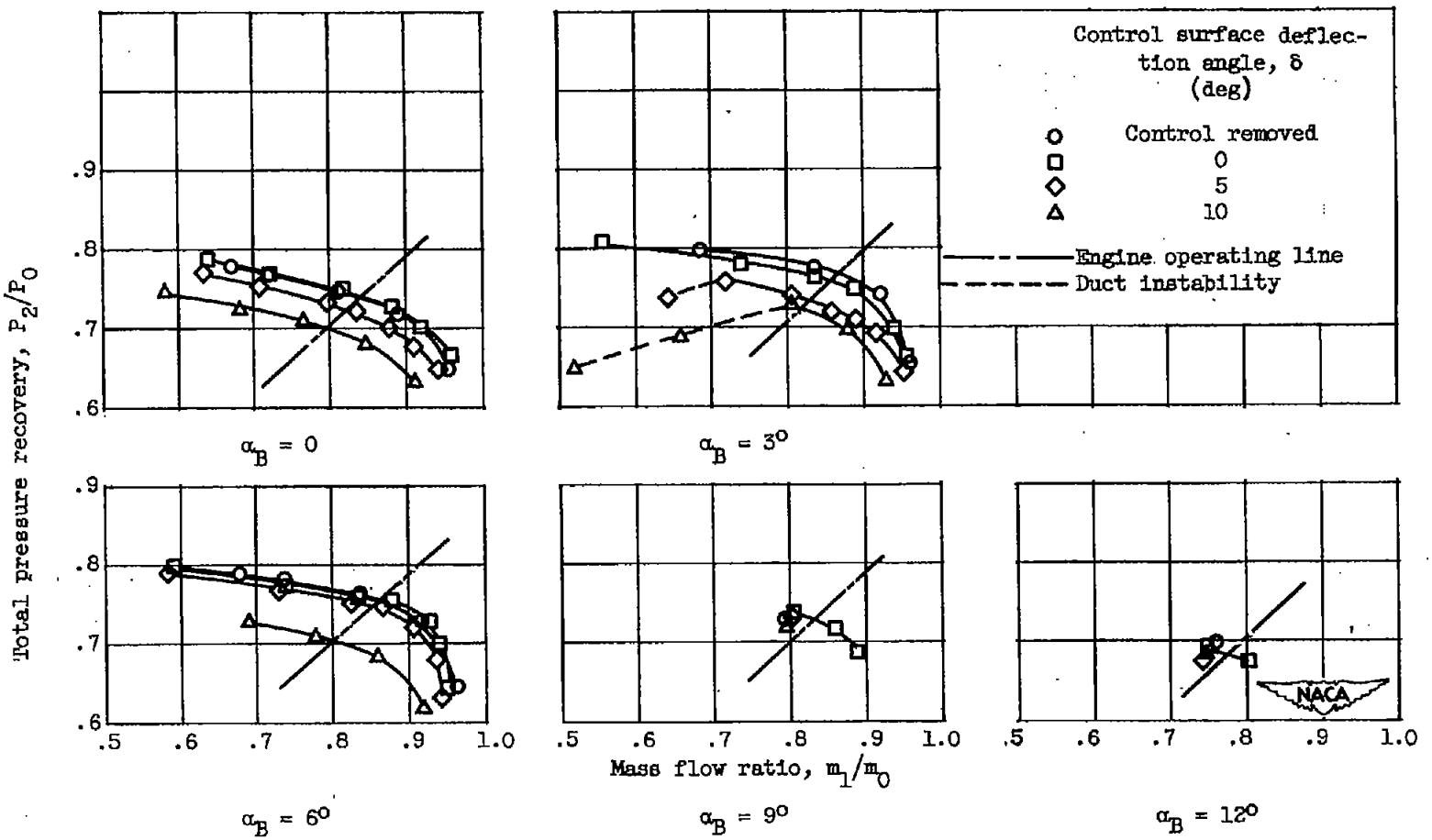

(b) Free-stream Mach number M_0, 1.8.

Figure 11. - Concluded. Total-pressure-recovery, mass-flow relationships for various control surface deflection angles. Angle of yaw Ψ, 0.

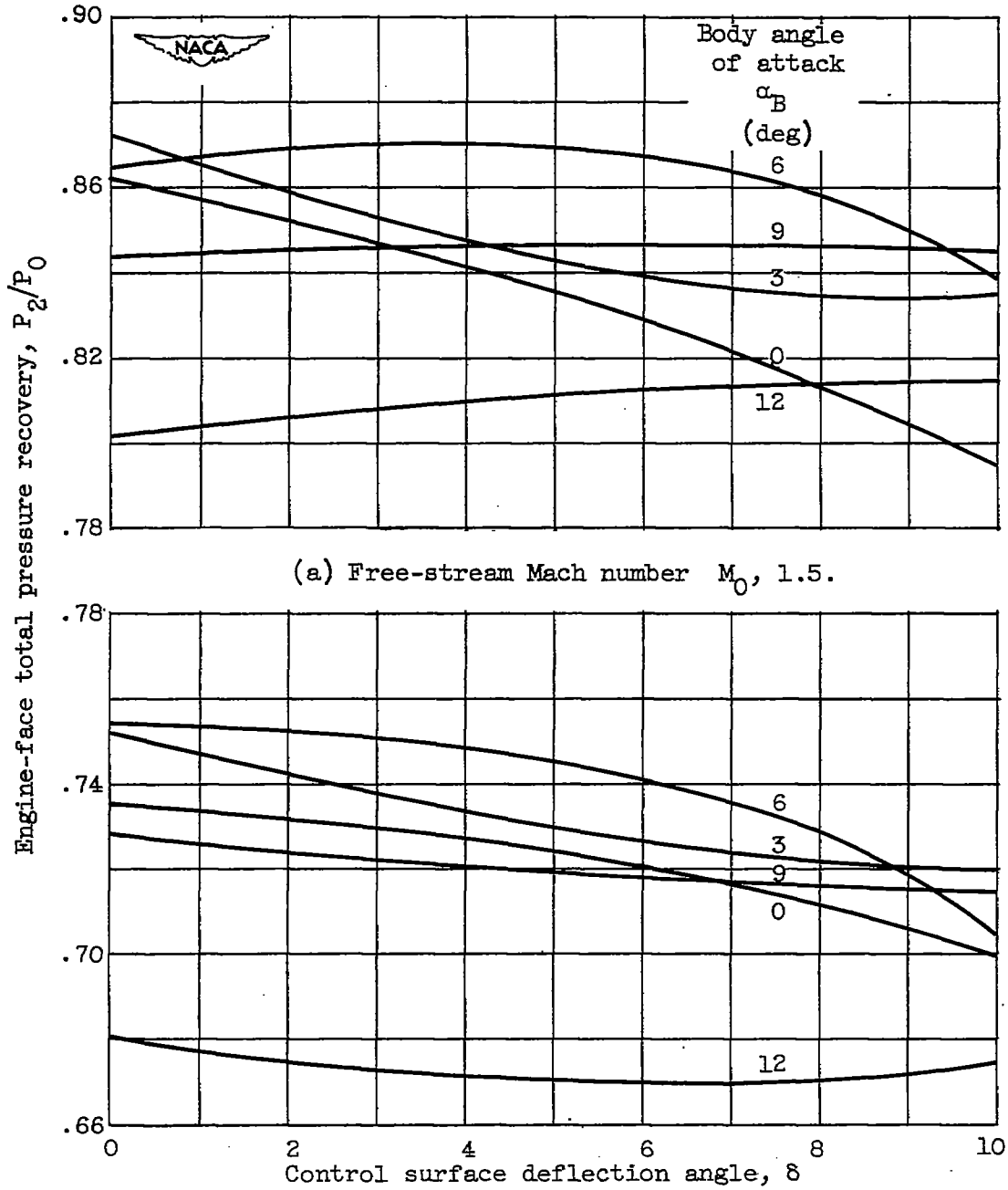

(a) Free-stream Mach number M_0, 1.5.

(b) Free-stream Mach number M_0, 1.8.

Figure 12. - Summary of effect of control surface deflection and body angle of attack on total pressure recovery at engine rated mass flow for hypothetical turbojet engine.

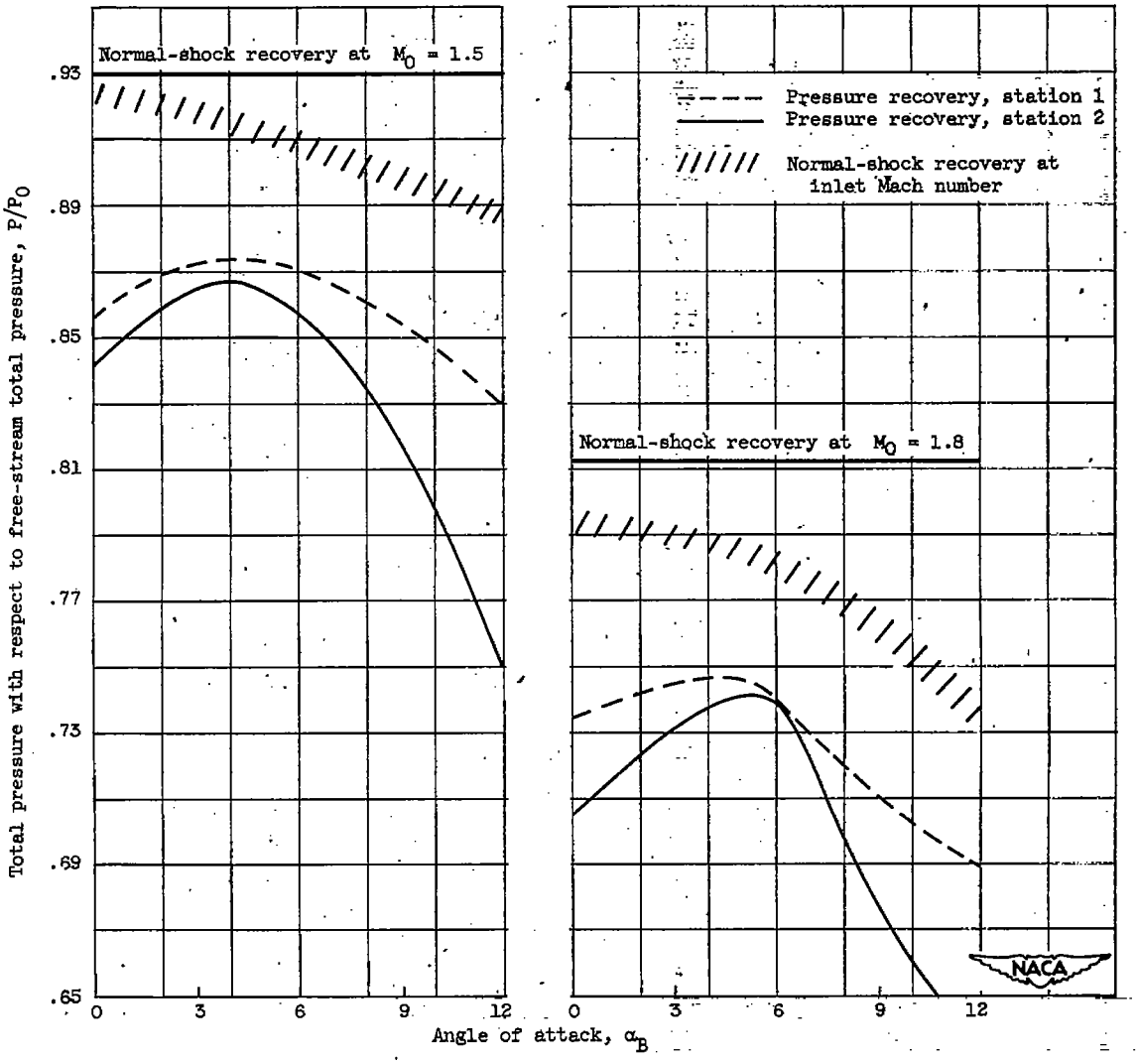

(a) Free-stream Mach number M_0, 1.5. (b) Free-stream Mach number M_0, 1.8.

Figure 13. - Breakdown of total pressure losses at mass flow ratio of 0.90. Control surface deflection δ, 0.

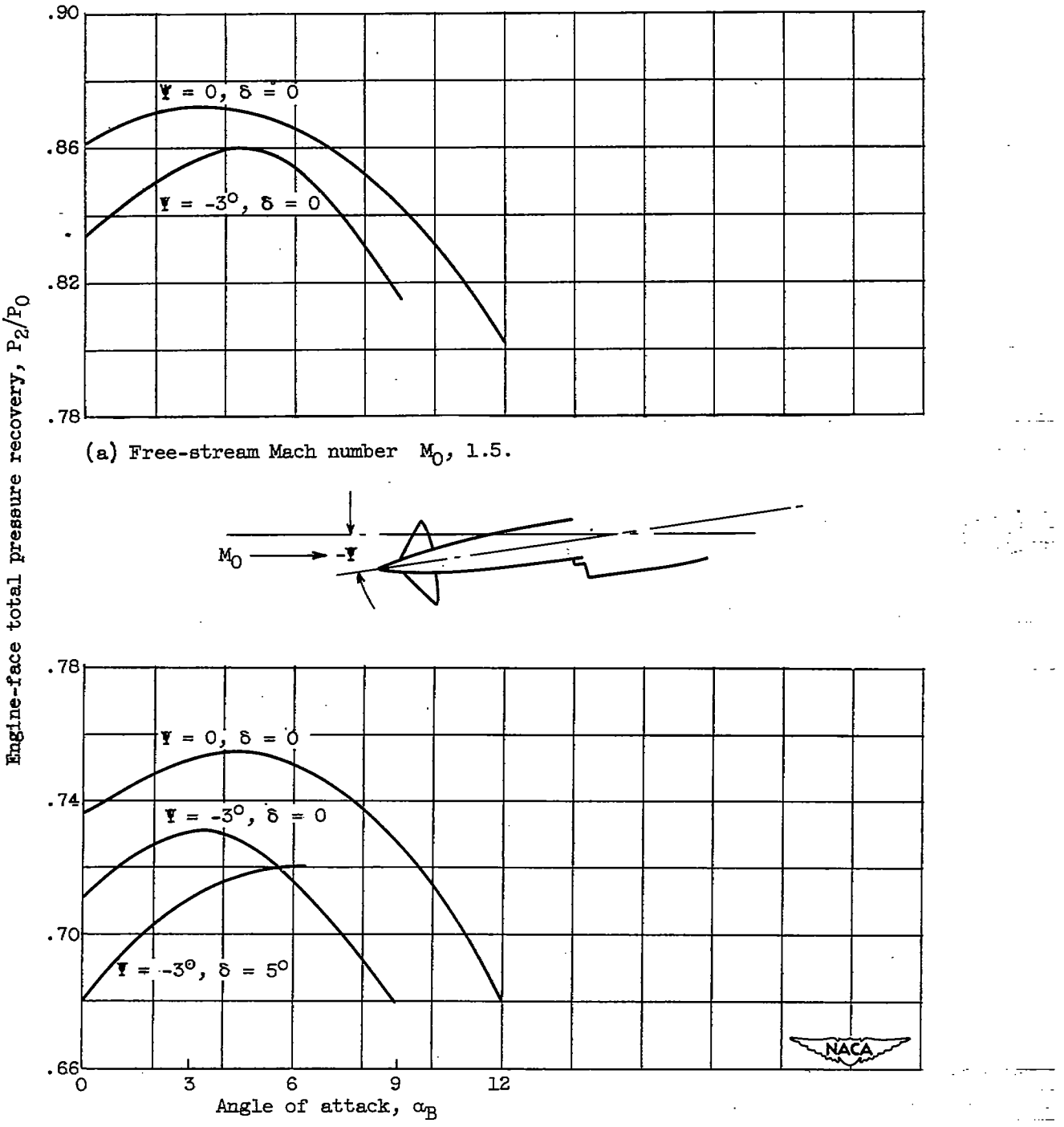

Figure 14. - Summary of yaw effect on total pressure recovery at engine rated mass flow for hypothetical turbojet engine.

NACA-Langley - 7-29-52 - 350